Impact of UV Radiation on the Raman Signal of Cystine: Implications for the Detection of S-rich Organics on Mars

V. Megevand, J.C. Viennet, E. Balan, Michel Gauthier, P. Rosier, M. Morand, Y. Garino, M. Guillaumet, S. Pont, O. Beyssac, et al.

ASTROBIOLOGY
Volume 21, Number 5, 2021

DOI: 10.1089/ast.2020.2340

Research Article

Impact of UV Radiation on the Raman Signal of Cystine: Implications for the Detection of S-rich Organics on Mars

V. Megevand,[1,2] J.C. Viennet,[1] E. Balan,[1] M. Gauthier,[1] P. Rosier,[1] M. Morand,[1] Y. Garino,[1] M. Guillaumet,[1] S. Pont,[1] O. Beyssac,[1] and S. Bernard[1]

Abstract

Traces of life may have been preserved in ancient martian rocks in the form of molecular fossils. Yet the surface of Mars is continuously exposed to intense UV radiation detrimental to the preservation of organics. Because the payload of the next rovers going to Mars to seek traces of life will comprise Raman spectroscopy tools, laboratory simulations that document the effect of UV radiation on the Raman signal of organics appear critically needed. The experiments conducted here evidence that UV radiation is directly responsible for the increase of disorder and for the creation of electronic defects and radicals within the molecular structure of S-rich organics such as cystine, enhancing the contribution of light diffusion processes to the Raman signal. The present results suggest that long exposure to UV radiation would ultimately be responsible for the total degradation of the Raman signal of cystine. Yet because the degradation induced by UV is not instantaneous, it should be possible to detect freshly excavated S-rich organics with the Raman instruments on board the rovers. Alternatively, given the very short lifetime of organic fluorescence (nanoseconds) compared to most mineral luminescence (micro- to milliseconds), exploiting fluorescence signals might allow the detection of S-rich organics on Mars. In any case, as illustrated here, we should not expect to detect pristine S-rich organic compounds on Mars, but rather by-products of their degradation. Key Words: Astrobiology—Organic degradation—Raman spectroscopy—Search for Mars' organics—Simulated martian UV radiation. Astrobiology 21, xxx–xxx.

1. Introduction

Today, the surface of Mars resembles a hyper-arid desert. This is in stark contrast to what is recorded in the late Noachian to early Hesperian rocks of the Southern Hemisphere: valley networks, paleolakes, and canyons all point to Mars being more habitable in its geological past (Fassett and Head, 2008; Grotzinger *et al.,* 2014; Wordsworth, 2016; Ramirez and Craddock, 2018). Because Mars currently lacks global plate tectonics, a unique record of ancient biological processes has thus possibly remained in the subsurface of Mars in the form of molecular fossils (McMahon *et al.,* 2018). Identifying on Mars the geological formations that potentially preserved organic biosignatures and studying them with appropriate instrumentation, both *in situ* and after their return to Earth, are now strategic priorities. This is why both NASA and ESA-Roscosmos are sending rovers to Mars (the NASA Mars 2020 Perseverance rover will land on Mars in February 2021, and the ESA-Roscosmos ExoMars Rosalind Franklin rover will take off in 2022), with the primary goal of searching for ancient traces of life likely under the form of organic compounds (Farley and Williford, 2017; Vago *et al.,* 2017).

Historically, no organic compounds were detected in martian soils by the pyrolysis gas chromatograph mass spectrometer (GCMS) on board the Viking landers besides small Cl-rich compounds which were interpreted back then as contamination (Biemann *et al.,* 1976, 1977). About 30 years later, the Phoenix lander reported the widespread presence of perchlorates (Hecht *et al.,* 2009), leading Navarro-González *et al.* (2010) to suggest that the Cl-rich compounds detected by the Viking landers were produced by reactions of martian organic materials with perchlorates during the pyrolytic measurements. This view has since been supported by laboratory experiments (Steininger *et al.,* 2012; Glavin *et al.,* 2013; Miller *et al.,* 2015; François *et al.,* 2016; Guzman *et al.,* 2018) and confirmed by the detection of Cl-rich organics by Sample Analysis at Mars (SAM), the

[1]Muséum National d'Histoire Naturelle, Institut de Minéralogie, Physique des Matériaux et Cosmochimie, CNRS UMR 7590, Sorbonne Université, Paris, France.
[2]Ecole Normale Supérieure de Lyon, Université Claude Bernard Lyon 1, Lyon, France.

pyrolysis GCMS on board Curiosity (Leshin *et al.,* 2013; Ming *et al.,* 2014; Freissinet *et al.,* 2015; Eigenbrode *et al.,* 2018; Szopa *et al.,* 2020). In addition, diverse pyrolysis products, including S-rich organics, were recently detected by SAM (Eigenbrode *et al.,* 2018), confirming the presence of organic compounds in the subsurface of Mars.

Still, the surface of Mars is known to be hostile for organic molecules: it is bombarded by ionizing radiation that can alter organic compounds (Fornaro *et al.,* 2018; Fox *et al.,* 2019). The thin CO_2 atmosphere of Mars absorbs most X-rays and far-UV radiation, but it lets mid- and near-UV photons in the range 190–410 nm, γ-rays, solar energetic protons, and galactic cosmic rays reach the surface (Patel *et al.,* 2002; Dartnell *et al.,* 2007; Hassler *et al.,* 2014). Even though UV photons do not penetrate that much below the surface (Carrier *et al.,* 2019), they can degrade organic compounds in timescales shorter than higher-energy particles capable of penetrating up to 2 m (days vs. hundreds of millions of years; Fornaro *et al.,* 2018; Fox *et al.,* 2019). Although UV radiation can be responsible for the production of photoresistant compounds in some cases (such as benzenehexacarboxylic acid-trianhydride; Stalport *et al.,* 2009), a number of studies, mostly relying on gas chromatography–mass spectrometry or Fourier transform infrared spectroscopy (FTIR), or both, have shown that the exposure to UV radiation leads to the rather fast photodecomposition of organic compounds (ten Kate *et al.,* 2005; Stalport *et al.,* 2009, 2019; Hintze *et al.,* 2010; ten Kate, 2010; Poch *et al.,* 2013, 2014; Fornaro *et al.,* 2018), which implies that the quest for organics relies on their preservation in deeper levels of the regolith. To this purpose, upcoming missions to Mars will embark Raman spectroscopy instruments (Abbey *et al.,* 2017; Rull *et al.,* 2017; Wiens *et al.,* 2017; Sapers *et al.,* 2019; Beyssac, 2020) combined with excavating tools. In the present study, we thus examine how S-rich organics such as cystine would react when freshly excavated and exposed to UV radiation, with a focus on the modifications of the Raman and luminescence signals.

2. Materials and Methods

2.1. Irradiation experiments

For the present study, we exposed pure cystine $(SCH_2CH(NH_2)CO_2H)_2$, Sigma-Aldrich, purity ≥98%, to UV radiation. Cystine is a dimer of amino acids and is composed of two cysteines linked by a disulfide bond. S-rich organics have been found on Mars (Eigenbrode *et al.,* 2018), and amino acids are common in chondrites (Kvenvolden *et al.,* 1970; Martins *et al.,* 2007, 2015), which justifies the selection of cystine for these experiments.

We used a mechanical press to form stubs of compressed polycrystalline samples (40 mg of cystine was pressed at 2 tons onto a stub 1 cm in diameter, leading to a final thickness of about 0.5 mm). Irradiation experiments were conducted in a dedicated Mars chamber built by the Cellule Projet @ Institut de Minéralogie, de Physique des Matériaux et de Cosmochimie (IMPMC) in which samples are exposed to UV radiation under controlled pressure and temperature conditions.

Here, experiments were conducted at 0°C under a primary vacuum. ten Kate *et al.* (2006) demonstrated that a martian atmosphere (6 mbar of CO_2) has no influence on the UV-induced degradation of amino acids. Thus, a martian-like CO_2 atmosphere was not introduced into the chamber to prevent absorption of UV by CO_2 and contamination from air. Samples were exposed to UV produced by a 150 W Xenon lamp (©LOT-ORIEL). Of note, this is the exact same lamp on which the Mars Organic Molecule Irradiation and Evolution (MOMIE) setup relies (Stalport *et al.,* 2009, 2019; Poch *et al.,* 2013, 2014). This lamp delivers a UV spectrum (190–400 nm) with a pattern similar to that of the martian surface radiation spectrum (Patel *et al.,* 2002; Dartnell *et al.,* 2007; Hassler *et al.,* 2014) but with a higher flux (Stalport *et al.,* 2009, 2019; Poch *et al.,* 2013, 2014), which thereby accelerates processes compared to true martian conditions.

The Raman signatures and fluorescence lifetimes of cystine samples were measured before and after 10, 100, and 1000 min of exposure to UV radiation directly in the Mars chamber, that is, under the conditions of the irradiation experiments. After 1000 min of irradiation, samples were removed from the chamber and measured with attenuated total reflectance Fourier transform infrared (ATR-FTIR) and electron spin resonance (ESR) spectroscopies. The comparison with spectra of pristine cystine allowed for documentation of the impact of UV radiation of the chemical structure and radical content of this S-rich dimer of amino acids. Note that the contribution of the volume of irradiated cystine to the measured signals differed from one technique to another, challenging a straightforward comparison between the data.

2.2. Time-resolved Raman spectroscopy

The remote configuration of a customized time-resolved Raman and luminescence spectrometer built at IMPMC was used for the present study (Fau *et al.,* 2019). Relying on a conventional Schmidt-Cassegrain telescope (Celestron-C8 ∼ 202 mm diameter Schmidt plate), this instrument allows for Raman signal collection of pristine and irradiated samples without removing them from the chamber in which the irradiation experiments are conducted. The laser is a nanosecond-pulsed 532 nm diode-pumped solid-state (DPSS) laser (1.2 ns full width at half maximum [FWHM], 1 mJ per pulse) with a 10–2000 Hz repetition rate. The fine control and synchronization of both time delay and gating time of the camera allows sub-nanosecond time resolution experiments.

For the present study, the laser was collimated at the sample surface (at 8 m from the telescope Schmidt plate) on a spot of ∼6 mm diameter, corresponding to a preservative irradiance of about $\sim 10^{10}$ W · m^{-2} (Fau *et al.,* 2019). The Raman signal was collected by the telescope from a surface with a slightly lower diameter than the co-aligned incident laser beam. A Notch filter was used to cut off the Rayleigh scattering below ∼90 cm^{-1}, and the signal was collected by an optical fiber and sent into a modified Czerny-Turner spectrometer (Princeton IsoPlane 320) coupled with a Princeton PIMAX4 intensified charge-coupled device (ICCD) camera. This spectrometer has three motorized gratings that can be selected depending on the spectral window and spectral resolution requested for the analysis.

We collected Raman and fluorescence signals using a 1.2 ns ICCD gate centered on the laser pulse. To maximize the signal-to-noise ratio, we accumulated the signals corresponding to

500,000 laser shots. The fluorescence lifetime of cystine samples (*i.e.,* the characteristic time spent by fluorescing centers to return from excited states to ground states; Beyssac 2020; Pasteris and Beyssac 2020) was investigated by collecting the background signal obtained and using a 1.2 ns ICCD gate for different delays after the laser pulse with a time resolution of 0.1 ns.

2.3. ATR-FTIR measurements

ATR-FTIR spectra of cystine samples were collected directly on the stubs, before and after exposure to UV radiation for 1000 min, over the 500–4000 cm^{-1} range with a 1 cm^{-1} resolution using a Nicolet 6700 FTIR spectrometer fitted with a KBr beam splitter and a detector for Fourier transform spectroscopy (DTGS)-KBr detector operating at IMPMC (Li *et al.,* 2014; Bernard *et al.,* 2015). The spectra shown here correspond to the average of 100 scans obtained in an attenuated total reflectance (ATR) geometry using a Specac Quest ATR device fitted with a diamond internal reflection element.

2.4. ESR measurements

ESR spectroscopy, also called electron paramagnetic resonance (EPR), allows for investigation of the presence of unpaired electrons and provides detailed information on structure bonding of paramagnetic species in samples exposed to ionizing radiation. ESR investigations were conducted at ambient temperature on powdered pristine cystine and cystine irradiated for 1000 min, using a BRUKER ESP 300E spectrometer operating at IMPMC (Sorieul *et al.,* 2005). Samples were filled in a pure silica tube (Suprasil grade), and the microwave power was set at 1 mW, while the amplitude and frequency of the magnetic field modulation were 0.5 mT and 100 kHz, respectively. The signal was collected over the 0.3200–0.3800 T range. The effective *g*-factor of the observed signals was determined by using the relation: $h\nu = g\beta H$ where ν is the microwave frequency, H the magnetic field, h the Planck constant, and β the Bohr magneton. A diphenyl-picryl-hydrazyle (DPPH, $g = 2.0037 \pm 0.0002$) standard was used for calibration.

3. Results

3.1. Raman spectroscopy and fluorescence

The Raman spectrum of pristine cystine exhibits a large number of bands that result from the stretching, bending, and rocking of O-C=O, C-S, C-H, and N-H bonds (Fig. 1). In particular, it displays a quite intense band at 499 cm^{-1} (Fig. 1) that results from the stretching of disulfide bridges (S-S bonds), an important component of the structure of proteins (Annis *et al.,* 1997). The exposure to UV does not lead to the appearance of any new Raman band. With increasing exposure to UV radiation, the continuous background contribution increases (by a factor of 5 after 1000 min of exposure to UV), while the intensities of the Raman bands of cysteine decrease (down to 1/3 of the initial intensities after 1000 min of exposure to UV) (Fig. 1). Such decrease in intensity appears similar for all modes, even though S-S bonds are known to be less strong/resistant than C-C and C-H bonds (Annis *et al.,* 1997; Nagy, 2013). Given the short time gate used in these experiments, the background signal may correspond to light diffusion processes related to disorder and/or to the intrinsic fluorescence of the cystine samples investigated. The intrinsic fluorescence of organic compounds (molecular fluorescence) represents a quantum process where an absorbed light quantum is re-emitted as light, generally at a different frequency (Weiss, 1943). In contrast to the signal that corresponds to light diffusion, which is contemporaneous of the laser pulse and can thus be modeled by a Gaussian function as a function of time, a fluorescence signal can be modeled by an exponential law as a function of time (Berezin and Achilefu, 2010). Here, the measured signal can be decomposed into a sum of a Gaussian function and an exponential function:

$$I(t) = I_{0.1} e^{-\left(\frac{t}{\tau_1}\right)^2} + I_{0.2} e^{\frac{-t}{\tau_2}} \quad (1)$$

with $I_{0.1}$ and $I_{0.2}$ the maximal intensity at $t = 0$ and τ_1 and τ_2 the lifetimes of the light diffusion and of the fluorescence signals. In such a scheme, the contribution of light diffusion to the measured signal corresponds to $I_{0.1} e^{-\left(\frac{t}{\tau_1}\right)^2} / I(t)$. Results show that, with increasing duration of exposure to UV radiation, the contribution of light diffusion to the signal increases significantly (from 60% of the total signal for the pristine cystine up to 93% for the cystine irradiated for 1000 min), indicating an increasing disorder (Fig. 2). In contrast, the signal that corresponds to the intrinsic fluorescence of cystine remains the same regardless of the exposure to UV radiation (Fig. 2), with a lifetime of about 4.4 ns, a value similar to that of other amino acids like tyrosine and tryptophan (Berezin and Achilefu, 2010). The fluorescence that contributes to the signal is likely emitted by the pristine cystine that lies below the irradiated sample surface (*cf,* Section 4.1).

3.2. Complementary characterization using ATR-FTIR and ESR spectroscopy

Irradiated cystine samples were removed from the chamber after exposure to UV to be measured by FTIR and ESR spectroscopies. The FTIR spectrum of pristine cystine exhibits a number of sharp and intense peaks below 1800 cm^{-1} as well as some large and less intense bands above 2000 cm^{-1}, attributed to the stretching, bending, and rocking of S-S, O-C=O, C-S, C-H, and N-H bonds (Fig. 3; Li *et al.,* 2014; Bernard *et al.,* 2015). All these features are still present in the spectrum of cystine irradiated for 1000 min, and no new feature is noticed (Fig. 3). Still, exposure to UV radiation impacted the shape of the absorption features: irradiated cystine exhibits less intense but broader signals than pristine cystine (Fig. 3). For instance, the intensity of the peak at 539 cm^{-1}, attributed to the rocking mode of O-C=O bonds, is 4 times higher for pristine cystine, while its FWHM is 2 times larger for irradiated cystine.

The ESR spectra of irradiated cystine mostly display two overlapping anisotropic signals (Fig. 4) similar to those previously observed by Thomsen and Nielsen (1972) in UV-irradiated cystine dihydrochloride. Radical I displays the following principal values of the *g*-tensor: $g_x = 2.052$, $g_y = 2.027$, and $g_z = 2.004$; while radical II is characterized by $g_x = 2.060$, $g_y = 2.034$, and $g_z = 1.995$ (Fig. 4). Although

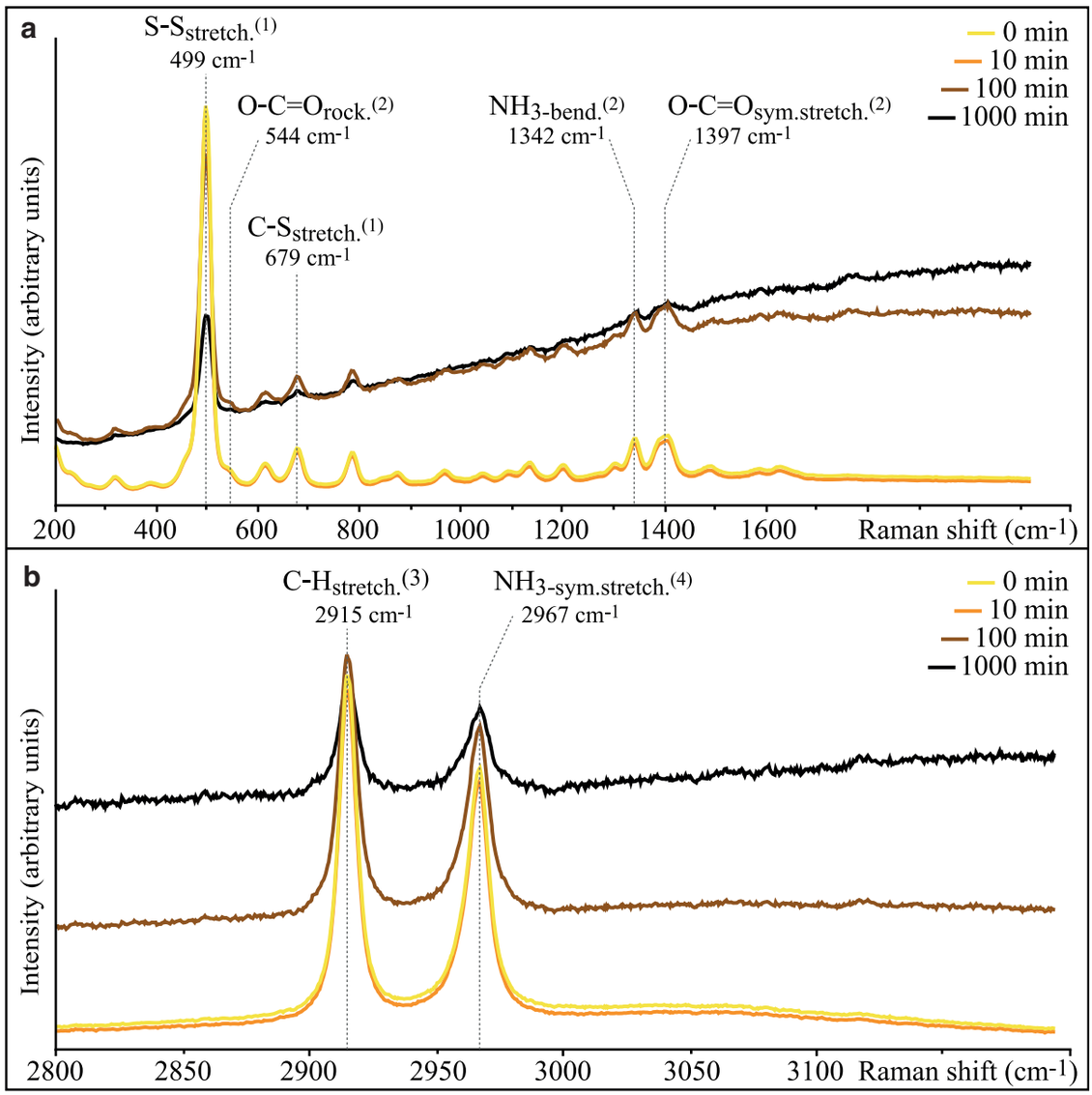

FIG. 1. Raman spectra centered at 1200 (**a**) and 3000 (**b**) cm^{-1} of pristine cystine and cystine irradiated for 10, 100, and 1000 min. Note that spectra were not shifted in intensity (*y* axis). The indexation of Raman bands is based on (1) Zhu *et al.,* 2011; (2) Pawlukojć *et al.,* 2005; (3) Jenkins *et al.,* 2005; and (4) Xie *et al.,* 2009. Color images are available online.

radical I was initially ascribed to a monosulfide species, further investigations (Hadley and Gordy, 1974; Nelson and Symons, 1975) and modeling (Engström *et al.,* 2000) have indicated that these two radicals correspond to paramagnetic disulfide species. The spectrum of pristine cystine displays similar paramagnetic signals at lower intensity. The shape of this spectrum, however, differs from that of the irradiated sample, with an anisotropic broadening of the g_x components and a more pronounced contribution at $g_x = 2.065$. The observed changes of *g*-values could be related to modifications of the charge state (cationic, anionic, neutral) or geometric configuration of the molecular environment of disulfide bridges (Engström *et al.,* 2000). The ESR spectrum thus reveals a slightly different environment and an increase in the concentration of disulfide paramagnetic species in irradiated cystine (Fig. 4). Quantifying these concentration changes is unfortunately not possible here because the volume of sample effectively affected by the UV radiation remains difficult to determine.

4. Discussion

4.1. Impact of exposure to UV radiation

The Raman and FTIR spectra of cystine irradiated for 1000 min under Mars conditions still exhibit all the features observed in the Raman and FTIR spectra of pristine cystine (Figs. 1 and 3). Still, the multi-technique approach adopted for the present study demonstrates that exposure to UV radiation strongly impacts cystine samples by triggering the creation of defects and radicals within the molecular

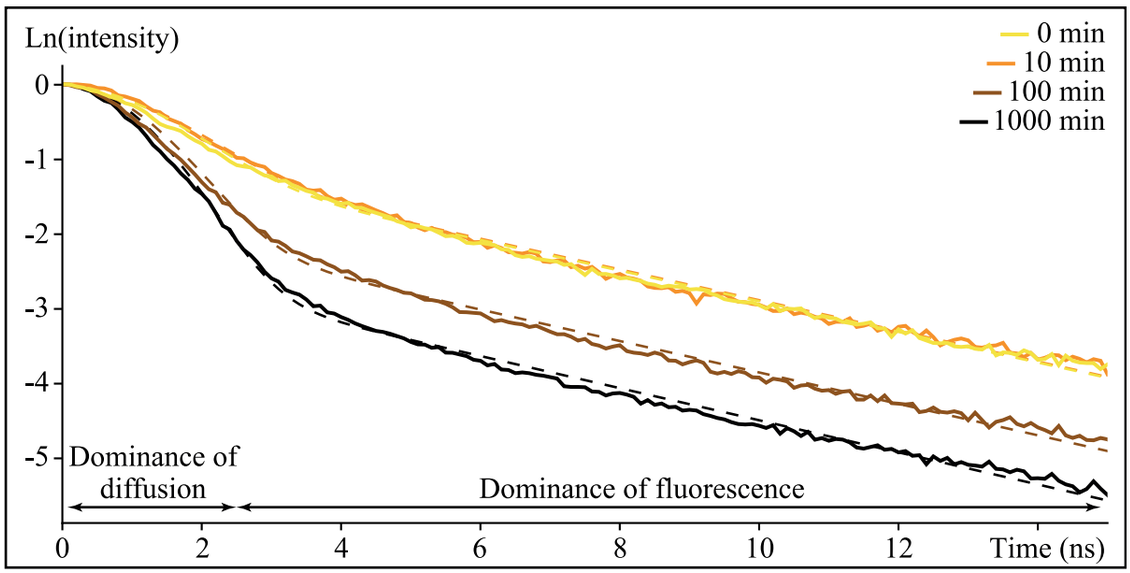

FIG. 2. Semi-log diagram of the signal intensity as a function of the time after the laser pulse for pristine and irradiated cystine samples. Data are normalized to their maximum intensity, and $t=0$ is defined for the maximum intensity of the signal. Dotted lines represent the model described in Eq.1. Fitted τ_1 values are 2 ns for pristine cystine and cystine irradiated for 10 min and 1.6 ns for cystine irradiated for 100 and 1000 min. Fitted τ_2 values are 4.4 ns for pristine cystine and cystine irradiated for 10 min and 4.3 ns for cystine irradiated for 100 and 1000 min. Color images are available online.

structure of cystine. The cystine samples turned yellow during exposure to UV radiation, which suggests the creation of defects or colored centers, or both, and potentially explains the evolution of Raman and FTIR signals. These defects do not seem to be fluorescing centers; in such a case, one would expect an increasing contribution of fluorescence to the collected Raman signal with increasing duration of exposure to UV radiation (Winkler *et al.,* 1998; Dumeige *et al.,* 2004). Plus, concentration quenching would decrease the lifetime of fluorescence, as reported for both organic and

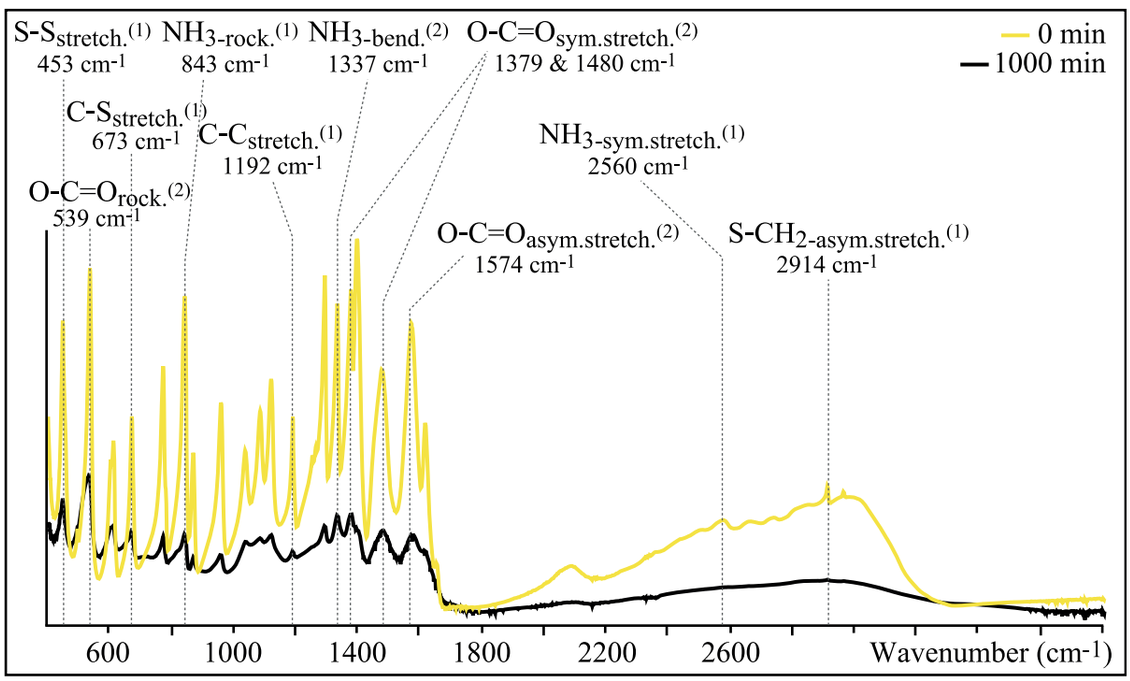

FIG. 3. ATR-FTIR spectra of pristine cystine and cystine irradiated for 1000 min. Note that spectra were not shifted in intensity (*y* axis). The indexation of infrared bands is based on (1) Zhu *et al.,* 2011; (2) Pawlukojć *et al.,* 2005. Color images are available online.

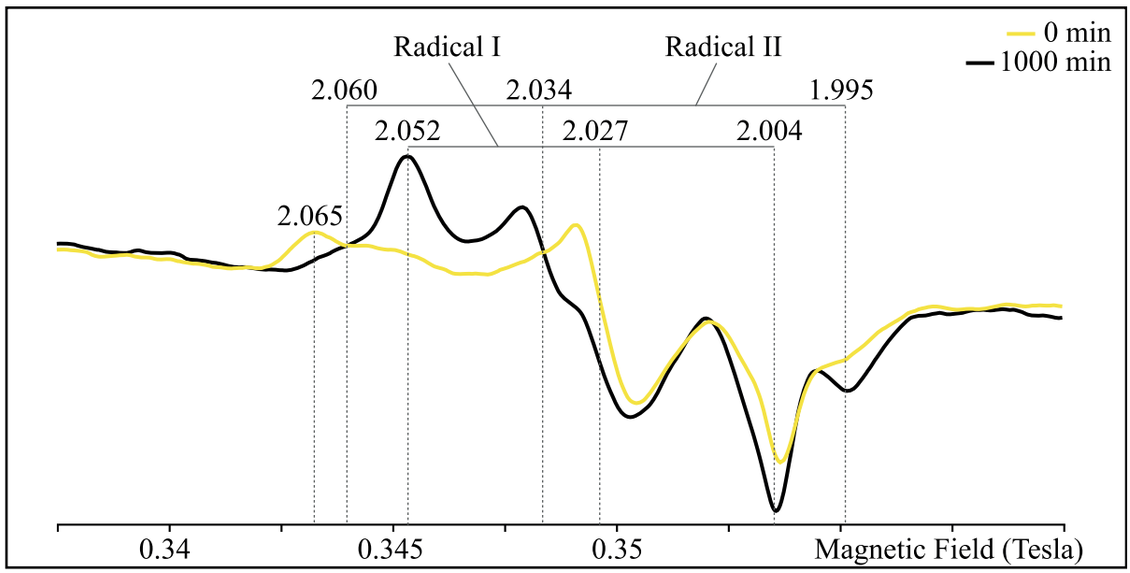

FIG. 4. ESR spectra of pristine cystine and cystine irradiated for 1000 min. Indexations correspond to the principal values of the *g*-tensor. Color images are available online.

inorganic materials (Chen and Knutson, 1988; Ju *et al.,* 2013; Meza *et al.,* 2014; Green and Buckley, 2015; Fau *et al.,* unpublished data), which is not the case here. Still, the broadening of Raman and FTIR bands is consistent with a higher concentration of point defects in irradiated cystine compared to pristine cystine (Fig. 3). Such broadening was previously reported in a number of materials exposed to ionizing radiation (*e.g.,* Fourdrin *et al.,* 2009). Consistently, the differences between the ESR spectra of pristine and irradiated cystine demonstrate that exposure to UV radiation was responsible for the creation/formation of a new population of radicals associated to disulfide bridges. Whether the radicals detected by ESR are the defects responsible for the broadening of Raman and FTIR bands remains difficult to determine, recalling that only the paramagnetic fraction of a defect population can be detected when using ESR. Obviously, quantitatively documenting the response of cystine to exposure to UV radiation will require monitoring the mass loss as a function of the dose.

4.2. Need for additional aging experiments

Our results suggest that long exposure to UV radiation would ultimately be responsible for the total degradation of the Raman signal of cystine. It follows that the detection of S-rich organics at the surface of Mars may be problematic, especially considering the many unknowns that remain. Here, we exposed crystalline cystine to UV radiation, but the response of amorphous cystine may be different. Also, as previously demonstrated, different organics do not react in similar ways when exposed to UV (ten Kate *et al.,* 2005; Stalport *et al.,* 2009, 2019; Hintze *et al.,* 2010; ten Kate, 2010; Poch *et al.,* 2013, 2014; Fornaro *et al.,* 2018). The effect of exposure to UV radiation on the Raman signal of other organic compounds thus will need to be further investigated. The same is true for the impact of other types of radiation. In fact, γ-rays, solar energetic protons, and galactic cosmic rays are not absorbed by the thin CO_2 atmosphere of Mars and can penetrate the martian subsurface to several meters of depth, potentially altering organic compounds (Kminek and Bada, 2006; Dartnell *et al.,* 2007; Hassler *et al.,* 2014; Fox *et al.,* 2019). In addition, because minerals may play a key role in the UV-induced degradation of organics (Poch *et al.,* 2015; dos Santos *et al.,* 2016; Ertem *et al.,* 2017; Fornaro *et al.,* 2018), it appears crucial to investigate the effects of mineral matrices typical of martian soils. Finally, many other aging processes likely act simultaneously at the surface of Mars, including oxidation (Lasne *et al.,* 2016) and degradation induced by fluid circulation (Viennet *et al.,* 2019). The impact of all these processes will have to be taken into account for the proper interpretation of future data.

4.3. Detection of S-rich organics on Mars using Raman

Here, we demonstrate that the detection of S-rich organics using Raman is achievable in freshly excavated martian samples, even though such samples would be quickly degraded by UV radiation. Note that the Raman instruments on board Perseverance and Rosalind Franklin will rely on different setups and strategies (Abbey *et al.,* 2017; Rull *et al.,* 2017; Wiens *et al.,* 2017; Sapers *et al.,* 2019; Beyssac, 2020). The RLS instrument on board Rosalind Franklin is a continuous Raman system that relies on a 532 nm laser, the SuperCam instrument on board Perseverance is a time-resolved Raman luminescence spectrometer that uses a pulsed 532 nm laser, and the SHERLOC instrument on board Perseverance will be a deep UV Raman and fluorescence spectrometer (Abbey *et al.,* 2017; Rull *et al.,* 2017; Wiens *et al.,* 2017; Sapers *et al.,* 2019; Beyssac, 2020). Here, we show that the Raman spectrum of cystine that has been exposed to UV radiation for a relatively short period of

time still exhibits the Raman spectral features of pristine cystine as well as a fluorescence signal that remains similar in intensity and lifetime. These results thus suggest that it should be possible to detect freshly excavated S-rich organics on Mars, that is, S-rich organics only exposed to UV for a short time, when using any of the Raman instruments on board the upcoming rovers, provided that such S-rich organics are present in concentrations above the detection limits and that the fluorescence of the mineral matrix does not dominate the signal. In addition, given the very short lifetime of the intrinsic molecular fluorescence of S-rich organics such as cystine (nanoseconds) compared to most mineral luminescence (micro- to milliseconds), SuperCam and SHERLOC may also be able to detect S-rich organics on Mars by exploiting fluorescence signals. In any case, we should not expect to detect pristine S-rich organic compounds on Mars, but rather by-products of their degradation.

Acknowledgments

We acknowledge the support of the IMPMC spectroscopy platform, and we thank Elisabeth Malassis (IMPMC) for administrative simplification. We acknowledge financial support from the program Emergences Alliance Sorbonne Université (Project MarsAtLab—PI: S. Bernard). The authors declare that there is no conflict of interest.

References

Abbey, W.J., Bhartia, R., Beegle, L.W., DeFlores, L., Paez, V., Sijapati, K., Sijapati, S., Williford, K., Tuite, M., Hug, W., *et al.* (2017) Deep UV Raman spectroscopy for planetary exploration: the search for *in situ* organics. *Icarus* 290:201–214.

Annis, I., Hargittai, B., and Barany, G. (1997) Disulfide bond formation in peptides. *Methods Enzymol* 289:198–221.

Berezin, M.Y. and Achilefu, S. (2010) Fluorescence lifetime measurements and biological imaging. *Chem Rev* 110:2641–2684.

Bernard, S., Benzerara, K., Beyssac, O., Balan, E., and Brown, G.E., Jr. (2015) Evolution of the macromolecular structure of sporopollenin during thermal degradation. *Heliyon* 1, doi:10.1016/j.heliyon.2015.e00034.

Beyssac, O. (2020) New trends in Raman spectroscopy: from high-resolution geochemistry to planetary exploration. *Elements* 16:117–122.

Biemann, K., Biller, J.A., Oro, J., Orgel, L.E., Nier, A.O., Anderson, D.M., Simmonds, P.G., Flory, D., Diaz, A.V., and Rushneck, D.R. (1976) Search for organic and volatile inorganic compounds in two surface samples from the Chryse Planitia region of Mars. *Science* 194:72–76.

Biemann, K., Oro, J., Toulmin, P., Orgel, L.E., Nier, A.O., Anderson, D.M., Simmonds, P.G., Flory, D., Diaz, A.V., Rushneck, D.R., *et al.* (1977) The search for organic substances and inorganic volatile compounds in the surface of Mars. *J Geophys Res* 82:4641–4658.

Carrier, B.L., Abbey, W.J., Beegle, L.W., Bhartia, R., and Liu, Y. (2019) Attenuation of ultraviolet radiation in rocks and minerals: implications for Mars science. *J Geophys Res Planets* 124:2599–2612.

Chen, R.F. and Knutson, J.R. (1988) Mechanism of fluorescence concentration quenching of carboxyfluorescein in liposomes: energy transfer to nonfluorescent dimers. *Anal Biochem* 172:61–77.

Dartnell, L.R., Desorgher, L., Ward, J.M., and Coates, A.J. (2007) Modelling the surface and subsurface martian radiation environment: implications for astrobiology. *Geophys Res Lett* 34, doi:10.1029/2006GL027494.

dos Santos, R., Patel, M., Cuadros, J., and Martins, Z. (2016) Influence of mineralogy on the preservation of amino acids under simulated Mars conditions. *Icarus* 277:342–353.

Dumeige, Y., Treussart, F., Alléaume, R., Gacoin, T., Roch, J.-F., and Grangier, P. (2004) Photo-induced creation of nitrogen-related color centers in diamond nanocrystals under femtosecond illumination. *J Lumin* 109:61–67.

Eigenbrode, J.L., Summons, R.E., Steele, A., Freissinet, C., Millan, M., Navarro-González, R., Sutter, B., McAdam, A.C., Franz, H.B., Glavin, D.P., *et al.*. (2018) Organic matter preserved in 3-billion-year-old mudstones at Gale Crater, Mars. *Science* 360:1096–1101.

Engström, M., Vahtras, O., and Ågren, H. (2000) MCSCF and DFT calculations of EPR parameters of sulfur centered radicals. *Chem Phys Lett* 328:483–491.

Ertem, G., Ertem, M.C., McKay, C.P., and Hazen, R.M. (2017) Shielding biomolecules from effects of radiation by Mars analogue minerals and soils. *Int J Astrobiol* 16:280–285.

Farley, K. and Williford, K. (2017) Seeking signs of life and more: NASA's Mars 2020 mission. *Eos* 98, doi:10.1029/2017EO066153.

Fassett, C.I. and Head, J.W. (2008) Valley network-fed, open-basin lakes on Mars: distribution and implications for Noachian surface and subsurface hydrology. *Icarus* 198:37–56.

Fau, A., Beyssac, O., Gauthier, M., Meslin, P.Y., Cousin, A., Benzerara, K., Bernard, S., Boulliard, J.C., Gasnault, O., Forni, O., *et al.*. (2019) Pulsed laser-induced heating of mineral phases: implications for laser-induced breakdown spectroscopy combined with Raman spectroscopy. *Spectrochim Acta Part B At Spectrosc* 160, doi:10.1016/j.sab.2019.105687.

Fornaro, T., Steele, A., and Brucato, J. (2018) Catalytic/protective properties of martian minerals and implications for possible origin of life on Mars. *Life* 8, doi:10.3390/life8040056.

Fourdrin, C., Balan, E., Allard, T., Boukari, C., and Calas, G. (2009) Induced modifications of kaolinite under ionizing radiation: an infrared spectroscopic study. *Phys Chem Mineral* 36:291–299.

Fox, A.C., Eigenbrode, J.L., and Freeman, K.H. (2019) Radiolysis of macromolecular organic material in Mars-relevant mineral matrices. *J Geophys Res Planets* 124:3257–3266.

François, P., Szopa, C., Buch, A., Coll, P., McAdam, A.C., Mahaffy, P.R., Freissinet, C., Glavin, D.P., Navarro-Gonzalez, R., and Cabane, M. (2016) Magnesium sulfate as a key mineral for the detection of organic molecules on Mars using pyrolysis. *J Geophys Res Planets* 121:61–74.

Freissinet, C., Glavin, D.P., Mahaffy, P.R., Miller, K.E., Eigenbrode, J.L., Summons, R.E., Brunner, A.E., Buch, A., Szopa, C., Archer, P.D., Jr., *et al.*; MSL Science Team. (2015) Organic molecules in the Sheepbed Mudstone, Gale Crater, Mars. *J Geophys Res Planets* 120:495–514.

Glavin, D.P., Freissinet, C., Miller, K.E., Eigenbrode, J.L., Brunner, A.E., Buch, A., Sutter, B., Archer, P.D., Jr., Atreya, S.K., Brinckerhoff, W.B., *et al.*. (2013) Evidence for perchlorates and the origin of chlorinated hydrocarbons detected by SAM at the Rocknest aeolian deposit in Gale Crater. *J Geophys Res Planets* 118:1955–1973.

Green, A.P. and Buckley, A.R. (2015) Solid state concentration quenching of organic fluorophores in PMMA. *Phys Chem Chem Phys* 17:1435–1440.

Grotzinger, J.P., Sumner, D.Y., Kah, L.C., Stack, K., Gupta, S., Edgar, L., Rubin, D., Lewis, K., Schieber, J., Mangold, N., *et al.*. (2014) A habitable fluvio-lacustrine environment at Yellowknife Bay, Gale Crater, Mars. *Science* 343, doi: 10.1126/science.1242777.

Guzman, M., McKay, C.P., Quinn, R.C., Szopa, C., Davila, A.F., Navarro-González, R., and Freissinet, C. (2018) Identification of chlorobenzene in the Viking gas chromatograph–mass spectrometer data sets: reanalysis of Viking mission data consistent with aromatic organic compounds on Mars. *J Geophys Res Planets* 123:1674–1683.

Hadley, J.H. and Gordy, W. (1974) Nuclear coupling of ^{33}S and the nature of free radicals in irradiated crystals of cystine dihydrochloride. *Proc Natl Acad Sci USA* 71:3106–3110.

Hassler, D.M., Zeitlin, C., Wimmer-Schweingruber, R.F., Ehresmann, B., Rafkin, S., Eigenbrode, J.L., Brinza, D.E., Weigle, G., Böttcher, S., Böhm, E., *et al.*. (2014) Mars' surface radiation environment measured with the Mars Science Laboratory's Curiosity rover. *Science* 343, doi:10.1126/science.1244797.

Hecht, M.H., Kounaves, S.P., Quinn, R.C., West, S.J., Young, S.M.M., Ming, D.W., Catling, D.C., Clark, B.C., Boynton, W.V., Hoffman, J., *et al.* (2009) Detection of perchlorate and the soluble chemistry of martian soil at the Phoenix lander site. *Science* 325:64–67.

Hintze, P.E., Buhler, C.R., Schuerger, A.C., Calle, L.M., and Calle, C.I. (2010) Alteration of five organic compounds by glow discharge plasma and UV light under simulated Mars conditions. *Icarus* 208:749–757.

Ju, G., Hu, Y., Chen, L., Wang, X., and Mu, Z. (2013) Concentration quenching of persistent luminescence. *Physica B: Condens Matter* 415:1–4.

Kminek, G. and Bada, J. (2006) The effect of ionizing radiation on the preservation of amino acids on Mars. *Earth Planet Sci Lett* 245:1–5.

Kvenvolden, K., Lawless, J., Pering, K., Peterson, E., Flores, J., Ponnamperuma, C., Kaplan, I.R., and Moore, C. (1970) Evidence for extraterrestrial amino-acids and hydrocarbons in the Murchison meteorite. *Nature* 228:923–926.

Lasne, J., Noblet, A., Szopa, C., Navarro-González, R., Cabane, M., Poch, O., Stalport, F., François, P., Atreya, S.K., and Coll, P. (2016) Oxidants at the surface of Mars: a review in light of recent exploration results. *Astrobiology* 16:977–996.

Leshin, L.A., Mahaffy, P.R., Webster, C.R., Cabane, M., Coll, P., Conrad, P.G., Archer, P.D., Atreya, S.K., Brunner, A.E., Buch, A., *et al.*; MSL Science Team. (2013) Volatile, isotope, and organic analysis of martian fines with the Mars Curiosity rover. *Science* 341, doi:10.1126/science.1238937.

Li, J., Bernard, S., Benzerara, K., Beyssac, O., Allard, T., Cosmidis, J., and Moussou, J. (2014) Impact of biomineralization on the preservation of microorganisms during fossilization: an experimental perspective. *Earth Planet Sci Lett* 400:113–122.

Martins, Z., Alexander, C.M.O., Orzechowska, G.E., Fogel, M.L., and Ehrenfreund, P. (2007) Indigenous amino acids in primitive CR meteorites. *Meteorit Planet Sci* 42:2125–2136.

Martins, Z., Modica, P., Zanda, B., and d'Hendecourt, L.L.S. (2015) The amino acid and hydrocarbon contents of the Paris meteorite: insights into the most primitive CM chondrite. *Meteorit Planet Sci* 50:926–943.

McMahon, S., Bosak, T., Grotzinger, J.P., Milliken, R.E., Summons, R.E., Daye, M., Newman, S.A., Fraeman, A., Williford, K.H., and Briggs, D.E.G. (2018) A field guide to finding fossils on Mars. *J Geophys R Planets* 123:1012–1040.

Meza, O., Villabona-Leal, E.G., Diaz-Torres, L.A., Desirena, H., Rodríguez-López, J.L., and Pérez, E. (2014) Luminescence concentration quenching mechanism in $Gd_2O_3:Eu^{3+}$. *J Phys Chem A* 118:1390–1396.

Miller, K.E., Kotrc, B., Summons, R.E., Belmahdi, I., Buch, A., Eigenbrode, J.L., Freissinet, C., Glavin, D.P., and Szopa, C. (2015) Evaluation of the Tenax trap in the Sample Analysis at Mars instrument suite on the Curiosity rover as a potential hydrocarbon source for chlorinated organics detected in Gale Crater. *J Geophys Res Planets* 120:1446–1459.

Ming, D.W., Archer, P.D., Glavin, D.P., Eigenbrode, J.L., Franz, H.B., Sutter, B., Brunner, A.E., Stern, J.C., Freissinet, C., McAdam, A.C., *et al.*. (2014) Volatile and organic compositions of sedimentary rocks in Yellowknife Bay, Gale Crater, Mars. *Science* 343, doi:10.1126/science.1245267.

Nagy, P. (2013) Kinetics and mechanisms of thiol–disulfide exchange covering direct substitution and thiol oxidation-mediated pathways. *Antioxidants & Redox Signaling* 18: 1623–1641.

Navarro-González, R., Vargas, E., de la Rosa, J., Raga, A.C., and McKay, C.P. (2010) Reanalysis of the Viking results suggests perchlorate and organics at midlatitudes on Mars. *J Geophys Res* 115, doi:10.1029/2010JE003599.

Nelson, D. and Symons, M.C.R. (1975) The detection of thiyl radicals by ESR spectroscopy. *Chem Phys Lett* 36:340–341.

Pasteris, J.D. and Beyssac, O. (2020) Welcome to Raman spectroscopy: successes, challenges, and pitfalls. *Elements* 16:87–92.

Patel, M.R., Zarnecki, J.C., and Catling, D.C. (2002) Ultraviolet radiation on the surface of Mars and the Beagle 2 UV sensor. *Planet Space Sci* 50:915–927.

Poch, O., Noblet, A., Stalport, F., Correia, J.J., Grand, N., Szopa, C., and Coll, P. (2013) Chemical evolution of organic molecules under Mars-like UV radiation conditions simulated in the laboratory with the ''Mars Organic Molecule Irradiation and Evolution'' (MOMIE) setup. *Planet Space Sci* 85: 188–197.

Poch, O., Kaci, S., Stalport, F., Szopa, C., and Coll, P. (2014) Laboratory insights into the chemical and kinetic evolution of several organic molecules under simulated Mars surface UV radiation conditions. *Icarus* 242:50–63.

Poch, O., Jaber, M., Stalport, F., Nowak, S., Georgelin, T., Lambert, J.-F., Szopa, C., Coll, P. (2015) Effect of nontronite smectite clay on the chemical evolution of several organic molecules under simulated martian surface ultraviolet radiation conditions. *Astrobiology* 15:221–237.

Ramirez, R.M. and Craddock, R.A. (2018) The geological and climatological case for a warmer and wetter early Mars. *Nat Geosci* 11:230–237.

Rull, F., Maurice, S., Hutchinson, I., Moral, A., Perez, C., Diaz, C., Colombo, M., Belenguer, T., Lopez-Reyes, G., Sansano, A., *et al.*; RLS Team. (2017) The Raman Laser Spectrometer for the ExoMars rover mission to Mars. *Astrobiology* 17, 627–654.

Sapers, H.M., Razzell Hollis, J., Bhartia, R., Beegle, L.W., Orphan, V.J., and Amend, J.P. (2019) The cell and the sum of its parts: patterns of complexity in biosignatures as revealed by deep UV Raman spectroscopy. *Frontiers in Microbiology* 10, doi:10.3389/fmicb.2019.00679.

Sorieul, S., Allard, T., Morin, G., Boizot, B., and Calas, G. (2005) Native and artificial radiation-induced defects in montmorillonite. An EPR study. *Phys Chem Mineral* 32:1–7.

Stalport, F., Coll, P., Szopa, C., Cottin, H., and Raulin, F. (2009) Investigating the photostability of carboxylic acids

exposed to Mars surface ultraviolet radiation conditions. *Astrobiology* 9:543–549.

Stalport, F., Rouquette, L., Poch, O., Dequaire, T., Chaouche-Mechidal, N., Payart, S., Szopa, C., Coll, P., Chaput, D., Jaber, M., *et al.* (2019) The Photochemistry on Space Station (PSS) experiment: organic matter under Mars-like surface UV radiation conditions in low Earth orbit. *Astrobiology* 19:1037–1052.

Steininger, H., Goesmann, F., and Goetz, W. (2012) Influence of magnesium perchlorate on the pyrolysis of organic compounds in Mars analogue soils. *Planet Space Sci* 71:9–17.

Szopa, C., Freissinet, C., Glavin, D.P., Millan, M., Buch, A., Franz, H.B., Summons, R.E., Sumner, D.Y., Sutter, B., Eigenbrode, J.L., *et al.* (2020) First detections of dichlorobenzene isomers and trichloromethylpropane from organic matter indigenous to Mars mudstone in Gale Crater, Mars: results from the Sample Analysis at Mars instrument onboard the Curiosity rover. *Astrobiology* 20:292–306.

ten Kate, I.L. (2010) Organics on Mars? *Astrobiology* 10:589–603.

ten Kate, I.L., Garry, J.R.C., Peeters, Z., Quinn, R., Foing, B., and Ehrenfreund, P. (2005) Amino acid photostability on the martian surface. *Meteorit Planet Sci* 40:1185–1193.

ten Kate, I.L., Garry, J.R.C., Peeters, Z., Foing, B., and Ehrenfreund, P. (2006) The effects of martian near surface conditions on the photochemistry of amino acids. *Planet Space Sci* 54:296–302.

Thomsen, E.L. and Nielsen, S.O. (1972) Electron spin resonance of single crystals of cystine dihydrochloride irradiated with monochromatic UV radiation at various wavelengths. *J Chem Phys* 57:1095–1099.

Vago, J.L., Westall, F., *et al.* (2017) Habitability on early Mars and the search for biosignatures with the ExoMars rover. *Astrobiology* 17:471–510.

Viennet, J.-C., Bernard, S., Le Guillou, C., Jacquemot, P., Balan, E., Delbes, L., Rigaud, B., Georgelin, T., and Jaber, M. (2019) Experimental clues for detecting biosignatures on Mars. *Geochemical Perspectives Letters* 12:28–33.

Weiss, J. (1943) Fluorescence of organic molecules. *Nature* 152:176–178.

Wiens, R.C., Maurice, S., and Rull Perez, F. (2017) The SuperCam remote sensing instrument suite for the Mars 2020 rover mission: a preview. *Spectroscopy* 32:50–55.

Winkler, E., Etchegoin, P., Fainstein, A., and Fainstein, C. (1998) Luminescence and resonant Raman scattering of color centers in irradiated crystalline L-alanine. *Phys Rev B* 57: 13477–13484.

Wordsworth, R.D. (2016) The climate of early Mars. *Annu Rev Earth Planet Sci* 44:381–408.

Address correspondence to:
S. Bernard
Muséum National d'Histoire Naturelle
Institut de Minéralogie, Physique des Matériaux et Cosmochimie
CNRS UMR 7590
Sorbonne Université
F-75005 Paris
France

E-mail: sbernard@mnhn.fr

Submitted 20 July 2020
Accepted 12 December 2020

Abbreviations Used

ATR = attenuated total reflectance
ESR = electron spin resonance
FTIR = Fourier transform infrared
FWHM = full width at half maximum
GCMS = gas chromatograph mass spectrometer
ICCD = intensified charge-coupled device
IMPMC = Institut de Minéralogie, de Physique des Matériaux et de Cosmochimie
SAM = Sample Analysis at Mars